Design of $Zn_{1-x}Cu_xO$ Nanocomposite Ag-doped As An Efficient Antibacterial Agent

maryam moosavifar (m.moosavifar90@gmail.com)

Department of Chemistry, Faculty of Science, University of Maragaheh, P.O. Box 55181-83111, Maragheh, Iran https://orcid.org/0000-0003-1538-8370

Golamreza Zarrini

Department of Animal Biology, Faculty of Natural Sciences, University of Tabriz, P.O. Box 51666-16471, Tabriz, Iran

Elnaz Mashmool Barjasteh

Department of Chemistry, Faculty of Science, University of Maragaheh, P.O. Box 55181-83111, Maragheh, Iran

Research Article

Keywords: Hybrid nanocomposite, Antibacterial agent, Ag-doping, Co-precipitation, Impregnation method

Posted Date: June 30th, 2021

DOI: https://doi.org/10.21203/rs.3.rs-657717/v1

Abstract

This study aims at the preparation of antimicrobial nanoparticles hybrid based on silver (Ag) doped $Zn_{1-x}Cu_xO$. $Zn_{1-x}Cu_xO$ nanocomposite Ag-doped prepared via wet chemical route, co-precipitation, and impregnation method, respectively. The inclusion of silver in the nanocomposite did not change its structure. However, the insertion of CuO into the ZnO structure has no impact due to the similarity of Cu ion radius with Zn ion radius (0.74 toward 0.73 Å). Hybrid nanomaterials characterized by XRD, FT-IR, and FESEM technique. The effect of loading of CuO nanoparticles into ZnO nanomaterials investigated on their antimicrobial behavior. For this purpose, CuO with a variety ratio doped on the ZnO nanoparticles, and then Ag entrapped by impregnation methods. Minimum inhibitory concentration (MIC) measurements were carried out to measure the antimicrobial behavior of ZnO(Ag) and mixed hybrid $Zn_{1-x}Cu_xO$(Ag) towards gram-negative and gram-positive bacteria and fungus. gram-positive and gram-negative bacteria were generally more sensitive to ZnO and CuO nanoparticles, respectively. Then, these hybrid nanomaterials can be an excellent candidate for both gram-positive and gram-negative bacteria.

Introduction

Nanotechnology is one of the most important areas that has been consideration recently because it provides the link between nanotechnology and nanobiotechnology. However, the combination of nanotechnology with nanobiotechnology leads to the development of new materials for therapeutic and diagnostic applications [1-3].

Besides, nanomaterials have numerous applications containing fuel cell, solar energy transformation, photonics, catalysis, optical biosensor, and photocatalysis that can be related to their unique physicochemical properties [4-7]. Moreover, these nanoporous materials are good candidates for antimicrobial agents. Metal oxides like inorganic nanomaterials have the properties of higher stability, low cost, and lower toxicity to human cells than other organic compounds [8-10].

Also, the problem of increasing microbial resistance to existing antibiotics makes inorganic materials similar to nanostructured metal oxides a worthy candidate for dissolve this problem [11].

The inhibition mechanism of nano-inorganic materials is through the production of toxins that enhanced oxidative stress and anti-inflammatory products, following in cell death. On the other hand, metal nanoparticles produce metal ions that capable of interaction with charged bacterial cell walls follow by the deactivation of cellular enzymes and lead to cell death [12-15]. Some nanometal oxides containing TiO_2, MgO, ZnO, CuO, and Fe_3O_4 nanoparticles were investigated as potential antimicrobial agents. Also, metal nanoparticles especially Ag nanoparticles were assigned more attention due to their exclusive biomedical properties such as wound dressing, cardiovascular implants, coating contact lenses, bone cement, bandages, and endodontic filling materials [16]. However, a mixed multi-metal oxide containing Ag/Fe_3O_4, $Zn_xMg_{1-x}O$, and Ta-doped ZnO has been studied as antimicrobial agents due to their synergic effects that reduce the high toxicity of alone nanoparticles [15, 17].

Mixed-metal oxide nanoparticles are preferred to the neat metal oxide nanoparticles in term of high toxicity and agglomeration. Many researchers have studied the effect of mixed-metal oxide nanoparticles on their cytotoxicity. These results were obtained with Zn doped CuO, Cu-doped TiO_2, Li-doped MgO, Zn doped MgO, Ti-doped MgO, $CuZnFe_2O_4$, Fe_3O_4, … [18-21]. It has been concluded the cytotoxicity of nanoparticles arises from two factors including releasing of the metal ion in media that causes their toxicity. This case observes in pure metal oxides such as ZnO and CuO. The second reason concerning the ROS (reactive oxygen species) detects in Co_3O_4 and Mn_3O_4 causes bacterial cell death. ROS is highly reactive oxygen such as H_2O_2, ·OH, $^1O_2$, and superoxide (O_2^-) that can be produced on the surface of metal oxide nanoparticles and can induce bacterial cell death [15].

Here, we aimed to report the preparation of the binary and ternary nanocomposite as antibacterial agents. This procedure achieves by modifying ZnO with CuO and Ag nanoparticles using the co-precipitation and impregnation method, respectively. After that, Ag^+ reduced by the use of hydrazine and obtained the new nanocomposite materials. CuO and ZnO showed antibacterial behavior against gram-negative and gram-positive bacteria, respectively. However, based on the formation of nanocomposite materials, synergic antibacterial properties against both gram-negative and gram-positive bacteria were observed. The effect of the ZnO/CuO ratio on antibacterial activity of the nano-composite has been investigated. However, Ag nanoparticles cause increasing in antibacterial activity. But it is expensive and high toxicity, but by inclusion in hybrid nanomaterials, the toxicity property reduced, and it appropriate from toxicity and economic view due to low loading. Besides, by the combination of them, the synergic effect of antibacterial properties appeared.

Experimental

2.1. Materials and Instruments

Materials commercially graded and purchased from Sigma-Aldrich, Fluka, and Merck. FT-IR spectra were recorded in the range 400–4000 cm^{-1} by a Thermo Nicolet Iso10 spectrometer by KBr pellets. UV-Vis spectrum detected by Shimadzu 1800 instrument. The morphology of the catalysts was studied using Field emission scanning electron micrographs (FESEM), which were recorded on a MIRA3 by Tuscan Co. To investigate catalysts from the structural view, a Brucker-D8 advance X-ray diffraction device with Cu-K_a radiation at λ=1.54 Å, v=40 kV, and I=30 mA in a range of 60-5° in ambient temperature detected. Azar Furnaces CVD apparatus was used for chemical deposition by a thermal method.

2.2. Preparation of ZnO nanoparticles

The preparation of ZnO nanoparticles performed by the wet-chemical method. For this purpose, a certain amount of $Zn(NO_3)_2$ (1mmol) was dissolved in 40 mL H_2O/ethanol with a 1:1 v/v ratio. Then, 1 g polyethylene glycol was added with stirring at 323 K for 30 min. Afterward, 2 g NaOH in 50 mL H_2O was added dropwise until milky gelatin formed. The ZnO NPs were collected by centrifugation, dried at 373 K for 1 hour, and were calcined at 673 K for 5 hours.

2.3. Preparation of $Zn_{1-x}Cu_xO$ nanoparticles

The preparation of $Zn_{1-x}Cu_xO$ nanoparticles achieved using the co-precipitation method. At first, different molar ratios (0.2/0.8, 0.4/0.6, 0.6/0.4, 0.8/0.2) of $Cu(NO_3)_2$ and $Zn(NO_3)_2$ was dissolved in 40 mL water/ethanol with 1:1 v/v ratio. The other stages are similar to the 2.2 section. After that, 1 g of polyethylene glycol was added and stirred for 30 min at 333 K. After that, 1 g of polyethylene glycol was added and stirred for 30 min at 333 K. Afterwards, the solution stirred at 333 K for 30 minutes. Finally, 2 g of NaOH was dissolved in 50 mL distilled water, added slowly to the solution until it was milky gel. The obtained materials were cooled, dried at 373 K for 1 hour, and calcined at 673 K for 5 hours.

2.4. Preparation of $Zn_{1-x}Cu_xO$(Ag) nanoparticles

Inclusion of Ag performed by conventional impregnation method. In this method, 2 g $Zn_{1-x}Cu_xO$ nanoparticles were suspended in a 100 mL aqueous solution of 0.1 M $AgNO_3$ and stirred at 323 K for 24 h. Then hydrazine was added slowly until the colour of the solution is changed. Then the obtained materials filtered, dried at 373 K, and calcined at 673 K for 5 hours.

2.5. Investigation of antimicrobial activity of nanoparticles

The antimicrobial activity of the hybrid nanomaterials was studied against the gram-negative bacteria *Salmonella enterica* (TUMC2131), *Escherichia coli* (PTCC1047), the gram-positive bacteria *Staphylococcus aureus* (PTCC1112), *Bacillus subtilis* (TUMC 1221), and a fungus *Candida Kefyr* (ATCC38296). Minimum inhibitory concentrations (MIC) of the nanomaterials were determined by CLSI broth microdilution method. In a 96-well plate, 200 µL Muller- Hinton broth medium for bacteria and Sabouraued`s dextrose broth medium for fungi were added to each well. Serial two-fold dilutions with the highest concentration of 100 µg/ml in the first well were prepared. The inoculums containing 10^4–10^5 colony-forming unit (CFU)/mL of the test microorganisms were added to each well. The plates were incubated at 310 K, for 18-24 hours for bacteria and at 298 K for fungus. The MICs were indicated as the lowest concentration of the nanomaterials capable of inhibiting growth the organisms in microdilution wells.

Result And Discussion

3.1. Synthesis and characterization of $Zn_{1-x}Cu_xO$(Ag)

Synthesis of $Zn_{1-x}Cu_xO$(Ag) hybrid nanocomposite performed using co-precipitation and impregnation methods, respectively. So, $Zn_{1-x}Cu_xO$ NPs are prepared by co-precipitation and then Ag embedded by the impregnation method. The reduction of Ag achieves by hydrazine, where hydrazine by manufacturing N_2 causes the production of inert media, therefore, it prevents re-oxidation of Ag [22]. However, hydrazine amount is used as stoichiometry until the reduction of Ag occurs not more.

Crystallinity and purity of the hybrids metal oxide NPs investigated by using XRD patterns. The marked diffraction peaks in the XRD pattern shows the polycrystalline nature of hybrid nanomaterials. Fig.1 shows the XRD pattern of mixed-metal oxide nanoparticles with the various ratio of Zn, Cu, and Ag. Fig.1a is the XRD pattern of ZnO(Ag) that indicated a peak in accordance with ZnO and Ag phases. Reflections according to Ag proved the formation of Ag nanoparticles into metal oxide. These reflections were appeared at 2q=38.11, 44.27, 64, and 77.8 with showed cubic crystal structure and lattice constant a=b=c=4.0862 Å [11]. In this regard, these reflections are related to Ag nanoparticles, not Ag_2O. This event can be related to the conversion of Ag cations to metallic Ag using hydrazine. However, peaks in relation to 2q= 32, 34.7, 36.2, 47.5, 57.1, 63, 66.5, 68.5, 69.1, and 73 correspond to (100), (002), (101), (102), (110), (103) and (112) planes of ZnO and indicating zincite phase of ZnO nanoparticles with hexagonal wurtzite structure and lattice constant is equal a=b=3.26 and c=5.21 Å [23, 24]. By doping Cu into ZnO structure by isomorphous substitution method, peaks in relation to CuO also begin to appear in the XRD pattern. The peak in accordance with CuO was appeared at 2q= 32, 36, 39, 46.5, 49, 54, 57, 67, 68.5, 73, and 75 is related to CuO nano metal oxide with a=b=c=3.597Å [22].

The low intensity of the CuO reflections in $Zn_{0.8}Cu_{0.2}O$(Ag) is due to the low loading of CuO, and based on increasing of CuO content, the intensity of related peaks increased. However, in these compounds, only reflections of Ag appeared, and no trace of Ag_2O observe. Also, no peak of Cu, Cu_2O, and Zn was observed that an indication of the usage of hydrazine in a stoichiometry amount. Furthermore, the inclusion of Cu is not affected the ZnO lattice. It is an expectable result because the ionic radius of Cu^{2+} (0.73) is nearly equal with Zn^{2+} (0.74), then Cu^{2+} can easily penetrate ZnO lattice without any distortion in the ZnO structure.

Fig.2 shows the IR spectra of ZnO(Ag) and $Zn_{1-x}Cu_xO$(Ag) nanocomposite dried at 673 K. According to Fig.2, observes bands in the region of 3000-3800 cm^{-1} and 480-1500cm^{-1}. The peaks of the region 798-1456 cm-1 are related to the organic compound that used as nanoparticles stabilizer and reduction reagent, which in turn, it is evident that vibration bands at 798, 1456, 1383, 1076, and 2168 cm^{-1} attributed to N-H, C-H, –C-O, -C-O-C, and C=C stretching modes, respectively. However, these bands were disappeared in some samples (b and c) which can be related to the calcination condition. Moreover, the absorbance band in the 3300 cm^{-1} is related to the O-H of water molecules attached to the nanoparticle surface by hydrogen bonding. Peaks in the region of 1632 cm^{-1} are in accordance with the bending vibration of H_2O molecules. However, the intensity of peaks in concern to organic compounds in ZnO (Ag) nanoparticles reduced that it can be related to the removing organic templates based on calcination.

The peaks concerning metallic Ag and Ag-Ag metallic bands establish below 400 cm^{-1} which cannot be seen in this spectrum because it is out of device range [11]. However, the sharp and strong peak between 400-600 cm^{-1} are according to ZnO nanoparticles overlapped with organic materials. Bands in relation to 472 and 515 cm^{-1} assigned to ZnO stretching vibration [23-25].

By inclusion CuO into the ZnO structure using the isomorphous substitution method, peaks in the region of 530-664 cm^{-1} appeared by CuO nanoparticles [26]. Based on increasing CuO content, its intensity increased, and the peak intensity of ZnO reduces which is an expected outcome and accompanied by slight shifting in peak location (Fig.2b). The FESEM images of ZnO(Ag) and $Zn_{1-x}Cu_xO$(Ag) nanoparticles revealed the polycrystalline structure (Fig.3). The presence of small crystallites with various sizes proved the formation of more than one phase and one crystalline structure. Furthermore, the morphology of ZnO(Ag) is different from $Zn_{1-x}Cu_xO$(Ag). ZnO(Ag) shows distinguished spherical morphology, although there are some nanoparticles with random form, and these results are concluded by others [27] that achieved by entering CuO and Ag in ZnO structure by isomorphism substitution and impregnation method, respectively.

3.2. Investigation of antimicrobial behavior of $Zn_{1-x}Cu_xO$(Ag) nanoparticles

Antibacterial activity of nanoparticles has been demonstrated by the MIC method (Table 1). For this purpose, gentamicin and nystatin were used as a bacterial control and nystatin and a fungal control, respectively. All nanoparticles had similar antibacterial behaviors relative to *Salmonella enterica*. Nanoparticles $Zn_{0.8}Cu_{0.2}O$(Ag), $Zn_{0.2}Cu_{0.8}O$(Ag), $Zn_{0.6}Cu_{0.4}O$(Ag) showed better antimicrobial behavior relative to nanoparticles $Zn_{0.4}Cu_{0.6}O$(Ag), ZnO(Ag) for *Staphylococcus aureus* and *Bacillus subtilis* and a *Candida Kefyr*. $Zn_{0.8}Cu_{0.2}O$(Ag) nanoparticles have better antibacterial behavior than the other nanoparticles for *Escherichia coli*. This is an expected result because CuO nanoparticles by affecting sulfide groups disturb enzyme function and inhibition of bacterial growth [28]. Therefore, there is a better antibacterial behavior against gram-positive bacteria *Staphylococcus aureus* and *Bacillus subtilis* and the *Candida Kefyr* fungal sample. Moreover, ZnO nanoparticles destroy the lipid the wall and protein of the cell membrane of the bacterium by producing H_2O_2 or electrostatic interaction between the bacteria and nanoparticles, which followed by the leakage of intracellular contents and ultimately the death of gram-negative bacterial cells, because the walls of bacterial cells of gram-negative is thinner than gram-positive [29, 30]. Nevertheless, ZnO (Ag) showed less antibacterial activity than $Zn_{1-x}Cu_xO$(Ag). It can be related to the size of ZnO which is reduced based on replacement with Cu and their antibacterial behavior increases [8]. Moreover, by introducing metallic silver based on its antibacterial nature, antibacterial behavior is superior against the gram-positive bacteria *Staphylococcus aureus* and *Bacillus subtilis* and the *Candida Kefyr* fungus than gram-negative bacterial. Then, by selecting the hybrid of nanoparticles we can tune the properties of NPs toward target particular virus/bacteria/microorganism, and therefore, we can achieve the tailor the sensitivity to a particular species.

Conclusions

The present study proposes the controlling of nanoparticle properties by changing their various ratios of ZnO and CuO. The change in reaction conditions led to the formation of different ratios of $Zn_{1-x}Cu_xO$(Ag) NPs. These results confirm by the XRD pattern. As the amount of ZnO reduces, the intensity of XRD peaks in accordance with it decreases and appeared peaks in relation to the CuO. In addition, peaks in relation

to the Ag nanoparticles appear in whole the samples due to the loading of Ag. By increasing in ZnO content, the antibacterial activity toward gram-positive increased, however in nanohybrid materials with a high loading of CuO, gram-negative antibacterial activity is enhanced. It is an acceptable result, because ZnO affected on the cell wall of the gram-positive bacterial. Besides, CuO via affecting on enzyme function causes cell death. Nevertheless, the presence of Ag nanoparticles affected both gram-positive and gram-negative bacteria and inhibition of the growth of the bacteria and fungus.

Declarations

Funding

Not applicable

Competing interests

The authors declare that they have no competing interests.

Availability of data and material

The datasets used and/or analysed during the current study are available from the corresponding author on reasonable request.

Code availability

Not applicable

Authors Contributions

M-Moosavifar conceived the study concept and designed experiments. E. Masmool synthesized nanocomposites. M-Moosavifar characterized the prepared samples. G. Zarrini investigated the antibacterial behavior of samples. M.Moosavifar and G. Zarrini wrote the manuscript. All authors read and approved the final manuscript.

Ethics approval

Authors declare this manuscript

The authors confirm the submission is original and they approved this manuscript is not under consideration for publication elsewhere.

Consent to participate

The authors are aware from their contribution in this paper.

Consent for publication

The authors are aware of the submission and agree to its publication. (include appropriate statemen

Acknowledgement

We wish to acknowledge the management of research and technology and the Central Laboratory of University of Maragheh for their help in running the experiments.

References

[1] K.A. Howard, J. Kjems, Expert opinion on biological therapy 7(12), 1811-1822 (2007).

[2] E.S. Andersen, M. Dong, M.M. Nielsen, K. Jahn, R. Subramani, W. Mamdouh, M.M. Golas, B. Sander, H. Stark, C.L. Oliveira, Nature 459(7243), 73 (2009).

[3] D. Bennett, D. Schuurbiers, NSTI Nanotech , 765-768 (2005).

[4] A.M.M. Jani, D. Losic, N.H. Voelcker, Progress in Materials Science 58(5), 636-704 (2013).

[5] C. De Montferrand, L. Hu, I. Milosevic, V. Russier, D. Bonnin, L. Motte, A. Brioude, Y. Lalatonne, Acta biomaterialia 9(4), 6150-6157 (2013).

[6] S.J. Ahmadi, M. Outokesh, M. Hosseinpour, T. Mousavand, Particuology 9(5), 480-485 (2011).

[7] A. Shalan, M. Rashad, Y. Yu, M. Lira-Cantú, M. Abdel-Mottaleb, Electrochimica Acta 89, 469-478 (2013).

[8] P. Joshi, S. Chakraborti, P. Chakrabarti, S.P. Singh, Z. Ansari, M. Husain, V. Shanker, Science of Advanced Materials 4(1), 173-178 (2012).

[9] J.S. Kim, E. Kuk, K.N. Yu, J.-H. Kim, S.J. Park, H.J. Lee, S.H. Kim, Y.K. Park, Y.H. Park, C.-Y. Hwang, Nanomedicine: Nanotechnology, Biology and Medicine 3(1), 95-101 (2007).

[10] P.K. Stoimenov, R.L. Klinger, G.L. Marchin, K.J. Klabunde, Langmuir 18(17), 6679-6686 (2002).

[11] L. Gharibshahi, E. Saion, E. Gharibshahi, A. Shaari, K. Matori, Materials 10(4), 402 (2017) .

[12] A.A. Tayel, W.F. EL-TRAS, S. Moussa, A.F. EL-BAZ, H. Mahrous, M.F. Salem, L. Brimer, Journal of Food Safety 31(2) 211-218 (2011).

[13] T. Takeshima, Y. Tada, N. Sakaguchi, F. Watari, B. Fugetsu, Nanomaterials 5(1), 284-297 (2015).

[14] A. Ivask, K. Juganson, O. Bondarenko, M. Mortimer, V. Aruoja, K. Kasemets, I. Blinova, M. Heinlaan, V. Slaveykova, A. Kahru, Nanotoxicology 8(sup1), 57-71 (2014).

[15] S. Stankic, S. Suman, F. Haque, J. Vidic, Journal of nanobiotechnology 14(1), 73 (2016).

[16] S. Chernousova, M. Epple, Angewandte Chemie International Edition 52(6), 1636-1653 (2013).

[17] A. Eremenko, N. Smirnova, I. Gnatiuk, O. Linnik, N. Vityuk, Y. Mukha, A. Korduban, Nanocomposites and Polymers with Analytical Methods. Rijeka: InTech, 51-83 (2011).

[18] Y. Rao, W. Wang, F. Tan, Y. Cai, J. Lu, X. Qiao, Applied Surface Science 284, 726-731 (2013).

[19] H.L. Karlsson, P. Cronholm, J. Gustafsson, L. Moller, Chemical research in toxicology 21(9) 1726-1732 (2008).

[20] J.C. Lai, M.B. Lai, S. Jandhyam, V.V. Dukhande, A. Bhushan, C.K. Daniels, S.W. Leung, International journal of nanomedicine 3(4), 533 (2008).

[21] M. Horie, K. Fujita, H. Kato, S. Endoh, K. Nishio, L.K. Komaba, A. Nakamura, A. Miyauchi, S. Kinugasa, Y. Hagihara, Metallomics 4(4), 350-360 (2012).

[22] S. Meghana, P. Kabra, S. Chakraborty, N. Padmavathy, RSC advances 5(16), 12293-12299 (2015).

[23] R. Hong, J. Li, L. Chen, D. Liu, H. Li, Y. Zheng, J. Ding, Powder Technology 189(3), 426-432 (2009).

[24] R. Dobrucka, J. Długaszewska, Saudi journal of biological sciences 23(4), 517-523 (2016).

[25] R. Yuvakkumar, J. Suresh, B. Saravanakumar, A.J. Nathanael, S.I. Hong, V. Rajendran, Spectrochimica Acta Part A: Molecular and Biomolecular Spectroscopy 137, 250-258 (2015).

[26] B.L. Rivas, E. Pereira, C. Guzmán, A. Maureira, Complexes of Water-Soluble Polymers with Cu^{2+} and Ag^{+} as Antibacterial Agents, Macromolecular Symposia, Wiley Online Library, 2011, pp. 46-54.

[27] P. Rajiv, S. Rajeshwari, R. Venckatesh, Spectrochimica Acta Part A: Molecular and Biomolecular Spectroscopy 112, 384-387 (2013).

[28] G. Ren, D. Hu, E.W. Cheng, M.A. Vargas-Reus, P. Reip, R.P. Allaker, International journal of antimicrobial agents 33(6), 587-590 (2009).

[29] M. Rai, A. Yadav, A. Gade, Biotechnology advances 27(1), 76-83 (2009).

[30] L. Zhang, Y. Jiang, Y. Ding, M. Povey, D. York, Journal of Nanoparticle Research 9(3), 479-489 (2007).

Tables

Table 1. The antibacterial activity of ZnO(Ag) and $Zn_{1-x}Cu_xO$(Ag) against gram-positive and gram-negative bacteria and fungus

compounds		*E.coli*	*S. enterica*	*S. aureus*	*B. subtilis*	*C. Kefyr*
1	$Zn_{0.4}Cu_{0.6}O$(Ag)	2000	2000<	2000	2000	2000
2	$Zn_{0.8}Cu_{0.2}O$(Ag)	1000	2000	1000	1000	1000
3	$Zn_{0.2}Cu_{0.8}O$(Ag)	2000	2000	1000	1000	1000
4	$Zn_{0.6}Cu_{0.4}O$(Ag)	2000<	2000<	1000	1000	1000
6	ZnO(Ag)	2000	2000	2000	2000	2000
Control		20	25	25	20	40

Figures

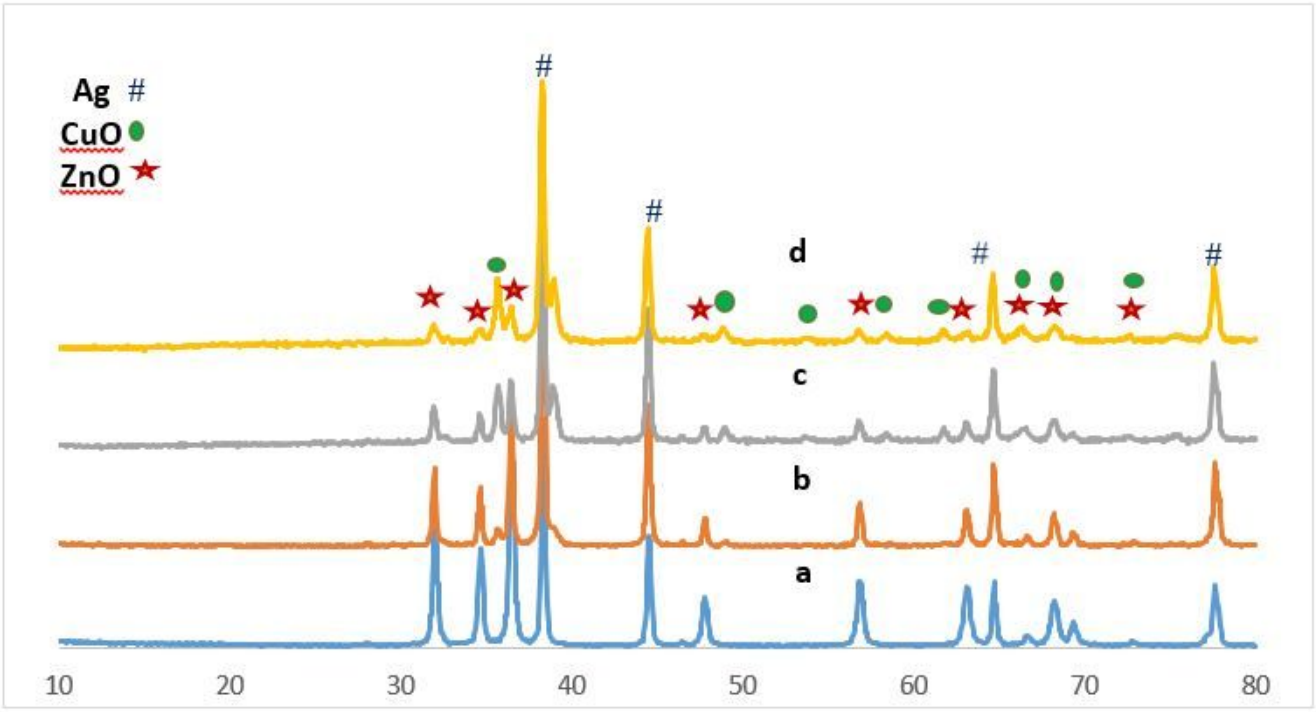

Figure 1

XRD pattern of a) ZnO(Ag), b) Zn0.8Cu0.2O(Ag), c) Zn0.4Cu0.6O(Ag), and Zn0.2Cu0.8O(Ag)

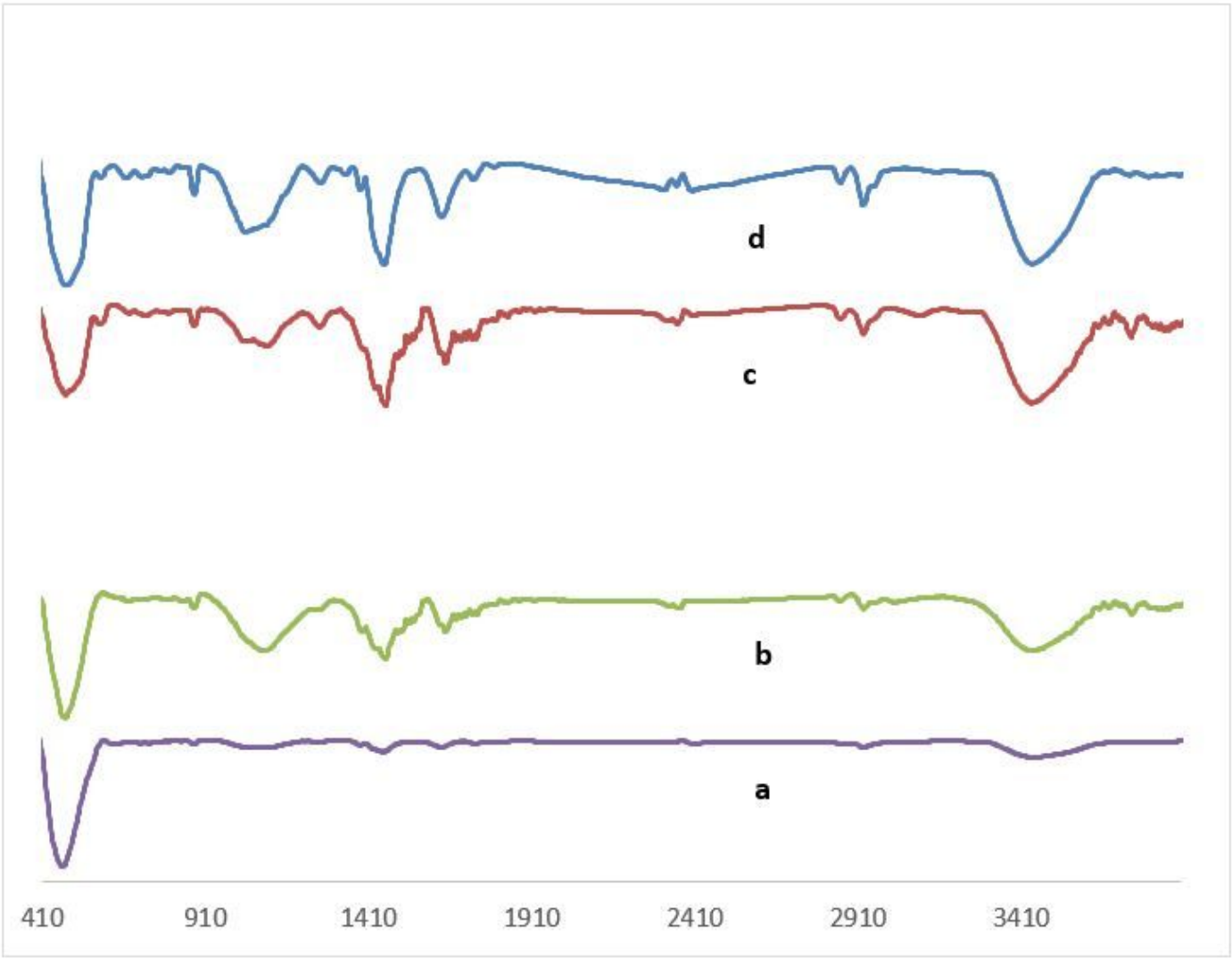

Figure 2

FT-IR spectrum of a) ZnO(Ag), b) Zn0.8Cu0.2O(Ag), c) Zn0.4Cu0.6O(Ag), and Zn0.2Cu0.8O(Ag)

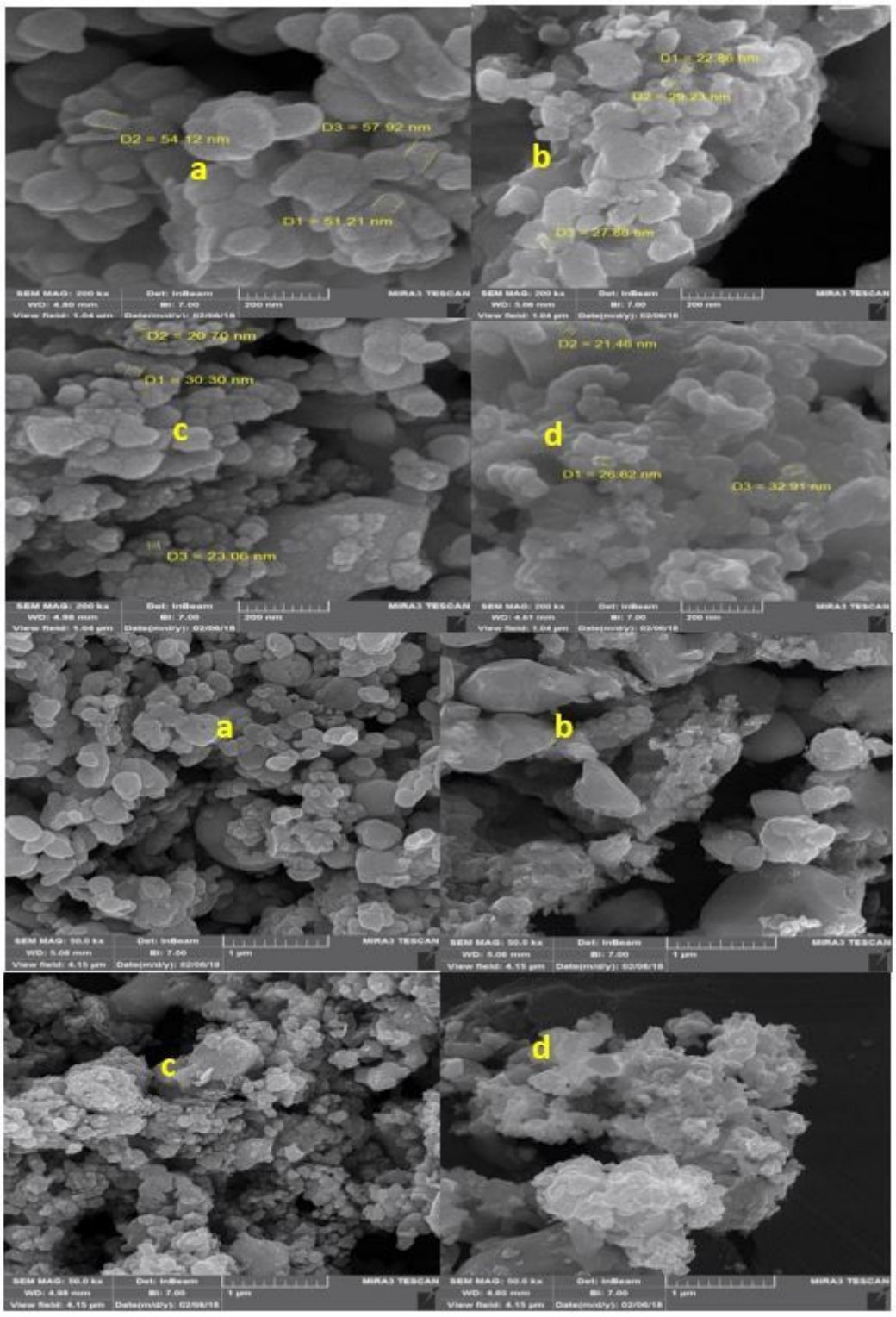

Figure 3

FESEM images with two magnitudes of a) ZnO(Ag), b) Zn0.8Cu0.2O(Ag), c) Zn0.4Cu0.6O(Ag), and Zn0.2Cu0.8O(Ag)